

# Screening of Phytochemicals from *Justicia Adhatoda* for Antitubercular Potential using Structure-Based Multitargeted Molecular Docking Analysis

Harsh Kashyap<sup>1</sup>, Gursimran Sekhon<sup>1</sup>, Manisha Khatri<sup>2,\*</sup> 

<sup>1</sup> Amity Institute of Biotechnology, Amity University, Noida, Uttar Pradesh

<sup>2</sup> Department of Biomedical Science, Shaheed Rajguru College of Applied Sciences for Women, University of Delhi

\* Correspondence: [manisha.khatri@rajguru.du.ac.in](mailto:manisha.khatri@rajguru.du.ac.in) (M.K.);

Scopus Author ID 35201066400

Received: 18.09.2023; Accepted: 12.05.2024; Published: 21.09.2024

**Abstract:** Tuberculosis remains a pressing global health concern, primarily driven by the dissemination of multi-drug resistant *M. tuberculosis* strains, necessitating the development of novel and more effective drugs. The present study aims to find bioactive antitubercular compounds by screening phytochemicals from the plant *Justicia adhatoda* using the multitargeted polypharmacology approach. Molecular docking studies of the phytochemicals were performed on four targets, PknB, InhA, MabA, and PanK, which are essential for the MTB cell wall biogenesis and physiological functions using AutoDock tools. The docking scores, drug-likeness, and toxicity studies found that Vitexin, Anisotine, Vasnetine, Apigenin, and Adhatodine are potential antitubercular compounds. Screening of phytochemicals from *J. adhatoda* against the critical target proteins led to the most promising therapeutic candidates against MTB. These findings are expected to contribute to traditional medicine-based therapy and the identification of potential candidates for future lead optimization in the development of antitubercular medications.

**Keywords:** *Justicia adhatoda*; antitubercular; molecular docking; polypharmacology; phytochemicals; virtual screening.

© 2024 by the authors. This article is an open-access article distributed under the terms and conditions of the Creative Commons Attribution (CC BY) license (<https://creativecommons.org/licenses/by/4.0/>).

## 1. Introduction

Tuberculosis (TB) is a contagious disease transmitted through air caused by the bacillus *Mycobacterium tuberculosis* (MTB). According to the World Health Organisation (WHO), TB is the second leading infectious killer after COVID-19 and the 13<sup>th</sup> leading cause of death worldwide. Additionally, it is the primary cause of mortality among individuals with HIV and a significant contributor to deaths associated with antimicrobial resistance. In 2021, an estimated 10.6 million people fell ill with TB worldwide, of which 6.7% accounted for people living with HIV. TB claimed the lives of 1.6 million individuals, with 187,000 of them also suffering from HIV. India is among the eight countries that account for two-thirds of the total global cases [1]. Numerous elements have played a role in the ongoing global health challenge posed by tuberculosis. This involves the development of drug resistance such as multidrug-resistant tuberculosis (MDR-TB), extensively drug-resistant tuberculosis (XDR-TB) [2], and totally drug-resistant tuberculosis (TDR-TB) [3]; the comorbidities with acquired immunodeficiency syndrome (AIDS) [4,5] and the risks involved in developing diabetes mellitus among TB patients [6,7]. The burden of drug-resistant TB (DR-TB) is also estimated

to have increased between 2020 and 2021, with 450000 new cases of rifampicin-resistant TB (RR-TB) in 2021.

Treatment for active TB is expensive and long, taking up to six months of daily doses of four first-line drugs: Isoniazid, rifampicin, ethambutol, and pyrazinamide, with almost an efficacy of 95% in susceptible individuals. But, the usage of these drugs is followed by a series of adverse side effects. The arena of anti-TB drug discovery has witnessed a lack of substantial active research for over four decades, even when currently available anti-TB drugs are deemed cytotoxic and have limited effectiveness due to the emergence of resistant bacterial strains [8]. The recent demand for the development of new and effective therapeutic agents to combat MDR, XDR, and TDR-TB has resulted in the identification of only a few potential anti-TB drug candidates [9]. Given the substantial rate of attrition experienced by drug candidates during clinical development, there is an urgent need to enhance and expand the exploration for new lead structures with anti-TB properties involving the utilization of validated mycobacterial drug targets. A promising emerging approach to overcoming drug-resistant TB is the polypharmacology approach, which includes developing a single molecule that can bind to multiple biological targets [10]. This approach has demonstrated promising results in terms of efficacy, synergistic effects, and adverse event prevention, as well as minimizing drug-drug interactions and the emergence of resistance. Hence, it is of utmost significance to uncover new chemical compounds with various action modes; medicinal plants may represent a potential option [11].

The design of novel anti-TB agents is focused on targeting various crucial enzymes responsible for Mycobacterium tuberculosis cell wall formation and essential physiological processes [12]. Protein kinase B (PknB) is one of the 11 Ser/Thr protein kinases of MTB and is responsible for phosphorylation-mediated signaling, mainly involved in cell wall synthesis, cell division, and metabolism [13]. Several studies have shown that its expression affects cell morphology and survival, with a depletion of PknB leading to the loss of bacterial viability [14-16] 2-trans-enoyl-ACP reductase (InhA) and  $\beta$ -ketoacyl-ACP reductase (MabA) are components of the type-II fatty acid elongation system (FAS-II). The latter comprises a complex ensemble of enzymes that play a crucial role in generating long-chain fatty acid derivatives that are critical precursors to mycolic acids, the primary constituents found in the cell wall of *M. tuberculosis*. [17,18]. The enzyme Pantothenate kinase (PanK, type I) is another target for developing novel anti-TB drugs, which plays a role in the synthesis of the Coenzyme A (CoA) cofactor from pantothenic acid, a vital component for the growth of *M. tuberculosis*. [19].

*Justicia adhatoda* L. belongs to the family Acanthaceae and is a shrub extensively distributed across Southeast Asia and the Indian subcontinent. The plant has anti-inflammatory, antispasmodic (bronchodilator), and expectorant properties [20], and its extract has traditionally been used to treat colds, coughs, asthma, and tuberculosis [21,22]. Our previous studies on *J. adhatoda* L. leaf extract have demonstrated anti-tubercular activity against *M. tuberculosis* MDR strains [23,24]. The main aim of this study is to screen the phytochemicals present in *Justicia adhatoda* using a molecular docking approach to develop an effective treatment for TB. The effectiveness of the screened compounds was validated based on the *in silico* docking technique by binding to the PknB, InhA, MabA, and PanK and ranked based on the interaction analysis between the protein receptor complex. In addition, the ADME and toxicity characteristics of the phytochemicals are also presented.

## 2. Materials and Methods

### 2.1. Design of database.

A comprehensive database of the phytoconstituents present in *J. adhatoda* encompassing a wide range of compounds including organo-sulfur compounds, alkaloids, alcohols, amino acids, flavonoids, fatty acids, fatty acid esters, steroids, carboxylic acids, esters, terpenes, saponins, phenols, and phenolic compounds was obtained from the Indian Medicinal Plants, Phytochemistry, and Therapeutics (IMPPAT) database for further *in silico* studies (<https://cb.imsc.res.in/imppat/phytochemical/Justicia%20adhatoda>).

### 2.2. Prediction of drug-like properties/(ADME analysis).

Estimating absorption, distribution, metabolism, and excretion (ADME) parameters through *in silico* methods relies on statistically derived models. In this study, the selected compounds were subjected to evaluation of their ADME parameters using the Swiss online ADME web tool [25,26]. Lipinski's rule of five for drug-likeness was also employed to assess the compounds' suitability as potential drugs [27].

### 2.3. Molecular docking.

AutoDock 4 and AutoDock tools were used for the *in silico* docking studies of the selected compounds [28]. The crystal structure of PknB (PDB ID: 2FUM), InhA (PDB ID: 1BVR), MabA (PDB ID: 1UZN), and PanK (PDB ID: 3AF3) were obtained from the RCSB protein data bank ([www.rcsb.org](http://www.rcsb.org)). Each crystal structure was individually prepared by eliminating existing ligands and water molecules. Missing hydrogens were added to the structure using AutoDock tools. Subsequently, non-polar hydrogens were merged, and polar hydrogens were incorporated into the protein file. The modified structure was saved in a docking-ready PDBQT format. For both standard and test compounds, the 2D chemical structures were obtained from PubChem, and they were further converted into their respective 3D conformations (mol2 format) using the Frog2 server [29]. Using AutoDock tools, the ligand molecules were converted and saved into the appropriate format for docking, namely the docking-ready PDBQT format [28]. AutoDock 4 was utilized to perform the docking process, where the ligands were docked with PknB, InhA, MabA, and PanK, and the binding affinities were subsequently determined. The selection of high-ranking small molecules was based on their binding position, potential interactions with key residues, and corresponding binding energy values obtained from AutoDock software. Conformations exhibiting the lowest binding affinities (less than -7.0 kcal/mol) were chosen for a closer examination of interacting residues. The docking poses were evaluated using Discovery Studio 2021 (Table 1).

**Table 1.** Grid box parameters are selected for the target enzyme based on the binding site residues.

Target Protein	Protein Description	PDB ID	Active Site Residues	Grid Box Parameters
PknB	Protein kinase B	2FUM	ASP36, TYR75, ASN67, TYR94, SER147, ALA148, ASP96	62.467 X 4.815 X -32.164
InhA	2-trans-enoyl-ACP reductase	1BVR	MET103, ALA198, ALA157, PRO156, PHE149, MET199	12.832 X 16.388 X 6.306
MabA	$\beta$ -ketoacyl-ACP reductase	1UZN	ARG25, ILE27, GLY28, GLY90, ALA89, ARG47, THR45	3.561 X 17.242 X 11.951

Target Protein	Protein Description	PDB ID	Active Site Residues	Grid Box Parameters
PanK	Pantothenate kinase	3AF3	LYS103, ARG238, TYR235, PHE239, ALA100, MET242, VAL99	-40.278 X 34.674 X -5.52

#### 2.4. Bioavailability radar and prediction of toxicity.

The drug-likeness of the candidates was thoroughly assessed, taking into account six physicochemical properties, including solubility, molecular size, polarity, lipophilicity, saturation, and flexibility. Additionally, the bioavailability radar was determined using the SwissADME tool [26]. All the compounds were evaluated *in silico* to predict the possible toxicity of these compounds using the “pkCSM” online computer program [30].

### 3. Results and Discussion

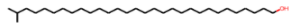
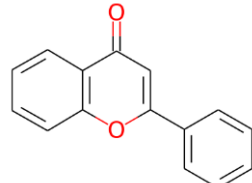
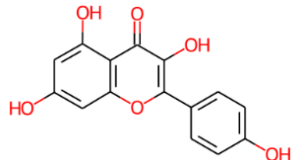
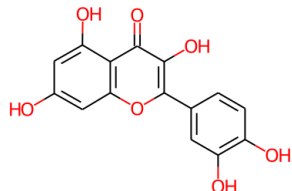
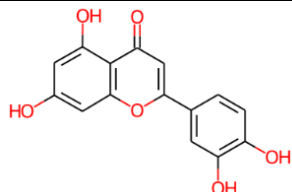
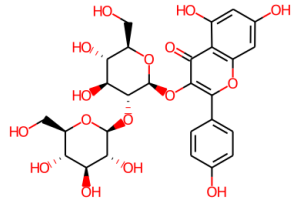
The concerning rise in strains of *Mycobacterium tuberculosis* (MTB) exhibiting multi-drug-resistant (MDR) and extensively drug-resistant (XDR) characteristics has driven the scientific community to explore novel, effective, and safer therapeutics. The current study mainly focuses on finding potential inhibitors of MTB using various computational tools. An attempt was made to explore various phytochemicals present in *J. adhatoda* against several proteins involved in MTB's progression and considered potential drug targets.

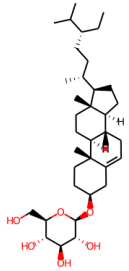
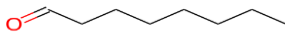

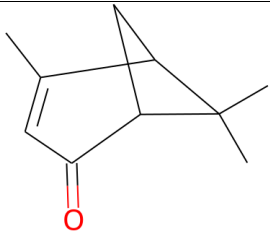
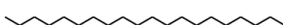
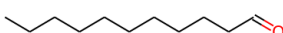


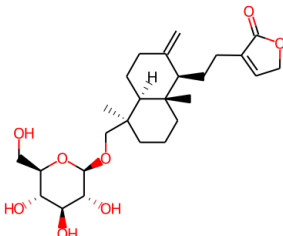
#### 3.1. Ligand selection.

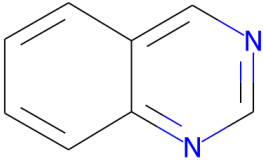
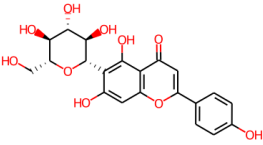







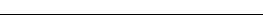

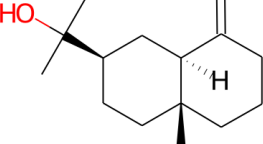
Molecules investigated in this study were selected from a diverse range of classes of phytochemicals, such as alkaloids, flavonoids, etc., from the plant *J. adhatoda*. The authors have proved that *J. adhatoda* leaf extracts have bioactive compounds with extensive antimycobacterial activity. The extract fractions inhibited the mycobacterium internalized in macrophages and synergy with the first-line anti-TB drug [24]. The current study examined 57 phytochemicals (Table 2 and Table 3) from the plant *J. adhatoda* obtained from the Indian Medicinal Plants, Phytochemistry, and Therapeutics (IMPPAT) database. Firstly, pharmacokinetic properties were evaluated, and Lipinski's rule of five was considered to assess the drug-likeness of molecules and predict toxicity (Table 2 and Table 3). Phytochemicals satisfying the Lipinski rule were considered for further analysis. Based on the binding affinity scores of the phytochemicals, the top 4 molecules with each receptor were chosen, resulting in the top 5 drug candidates, namely Vitexin, Anisotine, Vasnetine, Apigenin, and Adhatodine (Supplementary Table S1).

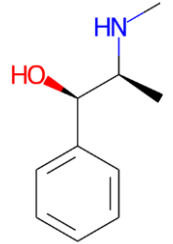
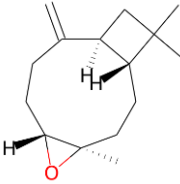
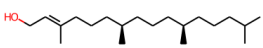
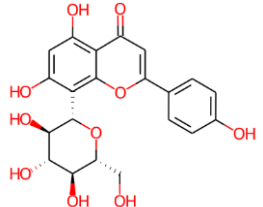
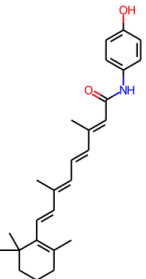
One of the most commonly utilized virtual screening techniques is molecular docking, which is employed to forecast the interaction between receptors and ligands. This approach has the capability to anticipate both the binding affinity and the structure of the protein-ligand complex, providing valuable insights for lead optimization [31]. The present study was performed to explore the affinity and binding interactions of the phytochemicals of *J. adhatoda* using Autodock in the active site of protein kinase B, 2-trans-enoyl-ACP reductase,  $\beta$ -ketoacyl-ACP reductase, and pantothenate kinase in search of the anti-tubercular compound. In order to validate the docking conditions prior to virtually screening the phytoconstituents, the control inhibitor was retrieved from its co-crystallized complex and re-docked using the AutoDock software against the relevant target.

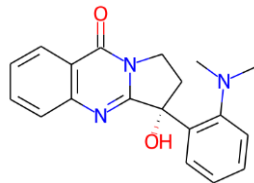
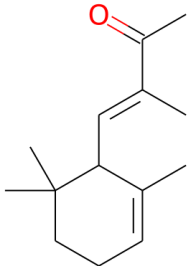
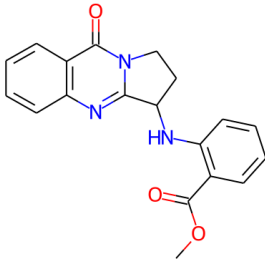
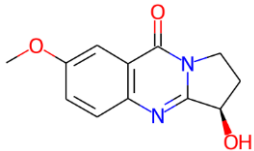
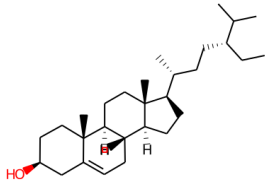
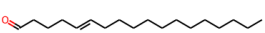
**Table 2.** ADME properties of the Phytochemicals of *Justicia adhatoda* predicted using the SwissADME online web server.

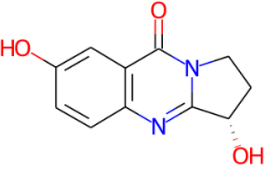
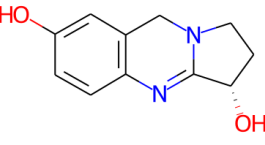
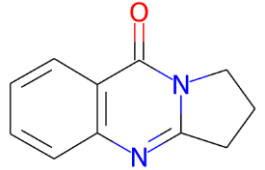
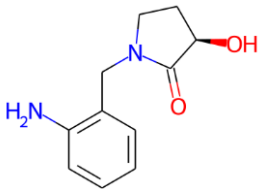
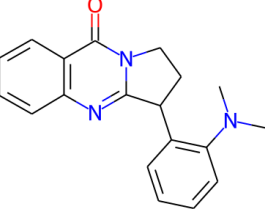
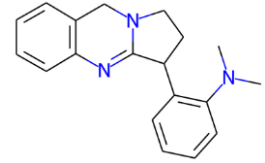
S.No	Compound	Structure	M. W.	Log P	HBA	HBD	TPSA	GI Abs	BBB
1	29-Methyl-1-triacontanol		452.84	11.17	1	1	20.23	Low	No
2	Flavone		222.24	3.46	2	0	30.21	High	Yes
3	Kaempferol		286.24	2.28	6	4	111.13	High	No
4	Quercetin		302.24	1.98	7	5	131.36	High	No
5	Luteolin		286.24	2.282	6	4	111.13	High	No
6	Sophoraflavonolside		610.52	2.420	16	10	269.43	Low	No

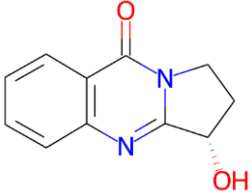
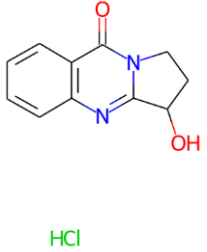
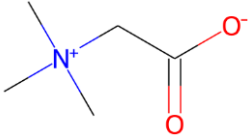
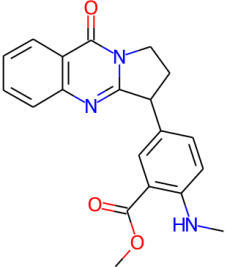
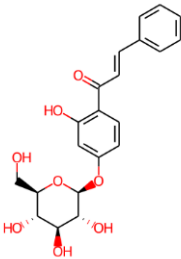
S.No	Compound	Structure	M. W.	Log P	HBA	HBD	TPSA	GI Abs	BBB
7	Daucosterol		576.85	5.849	6	4	99.38	Low	No
8	Octanal		128.21	2.545	1	0	17.07	High	Yes
9	Heptacosane		380.73	10.77	0	0	0	Low	No
10	Verbenone		150.22	2.177	1	0	17.07	High	Yes
11	Eicosane		282.55	8.048	0	0	0	Low	No
12	Undecanal		170.29	3.716	1	0	17.07	High	Yes
13	1-Tetradecanol		214.39	4.679	1	1	20.23	High	Yes
14	1-Octene		112.21	3.142	0	0	0	Low	Yes
15	Neoandrographolide		480.59	1.845	8	4	125.68	High	No

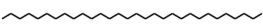
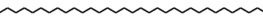
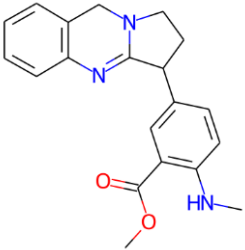
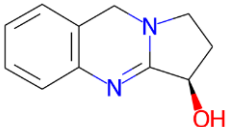
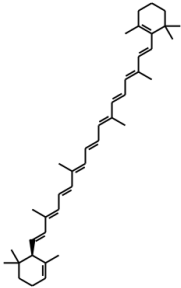
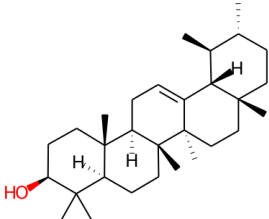
S.No	Compound	Structure	M. W.	Log P	HBA	HBD	TPSA	GI Abs	BBB
16	Quinazoline		130.15	1.629	2	0	25.78	High	Yes
17	Isovitexin		432.38	0.091	10	7	181.05	Low	No
18	Hentriacontane		436.84	12.33	0	0	0	Low	No
19	1-Pentadecanol		228.41	5.069	1	1	20.23	High	Yes
20	Pentacosane		352.68	9.998	0	0	0	Low	No
21	Heneicosane		296.57	8.438	0	0	0	Low	No
22	Nonacosane		408.79	11.55	0	0	0	Low	No
23	Tricosane		324.63	9.218	0	0	0	Low	No
24	Dodecane		170.33	4.9272	0	0	0	Low	No
25	Tetracontane		563.08	15.85	0	0	0	Low	No
26	Tetradecane		198.39	5.707	0	0	0	Low	No
27	beta-Eudesmol		222.37	3.92	1	1	20.23	High	Yes

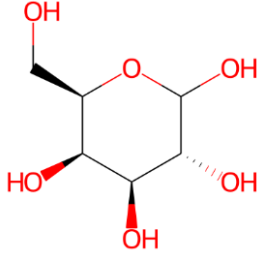
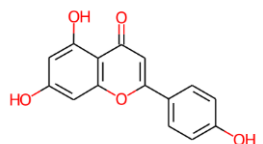
S.No	Compound	Structure	M. W.	Log P	HBA	HBD	TPSA	GI Abs	BBB
28	Ephedrine		165.23	1.327	2	2	32.26	High	Yes
29	Caryophyllene oxide		220.35	3.936	1	0	12.53	High	Yes
30	Phytol		296.53	6.364	1	1	20.23	Low	No
31	Vitexin		432.38	0.091	10	7	181.05	Low	No
32	Fenretinide		391.55	6.862	2	2	49.33	Low	No

S.No	Compound	Structure	M. W.	Log P	HBA	HBD	TPSA	GI Abs	BBB
33	Desmethoxyaniflorine		321.37	2.102	3	1	58.36	High	Yes
34	3-Methyl-4-(2,6,6-trimethyl-2-cyclohexen-1-yl)-3-buten-2-one		206.32	3.904	1	0	17.07	High	Yes
35	Vasnetine		335.36	2.74	4	1	73.22	High	Yes
36	7-Methoxyvasicinone		232.24	0.842	4	1	64.35	High	No
37	beta-Sitosterol		414.71	8.024	1	1	20.23	Low	No
38	5-Octadecenal		266.46	6.222	1	0	17.07	Low	No

S.No	Compound	Structure	M. W.	Log P	HBA	HBD	TPSA	GI Abs	BBB
39	Pyrrolo(2,1-b)quinazolin-9(1H)-one, 2,3-dihydro-3,7-dihydroxy-, (3S)-		218.21	0.539	4	2	75.35	High	No
40	Vasicinol		204.23	1.002	3	2	56.06	High	No
41	Deoxyvasicinone		186.21	1.342	2	0	34.89	High	Yes
42	Vasicol		206.24	0.362	2	2	66.56	High	No
43	Pyrrolo[2,1-b]quinazolin-9(1H)-one, 3-[2-(dimethylamino)phenyl]-2,3-dihydro-		305.37	2.998	2	0	38.13	High	Yes
44	Benzenamine, N,N-dimethyl-2-(1,2,3,9-tetrahydropyrrolo[2,1-b]quinazolin-3-yl)-		291.39	3.785	1	0	18.84	High	Yes

S.No	Compound	Structure	M. W.	Log P	HBA	HBD	TPSA	GI Abs	BBB
45	(3S)-3-hydroxy-2,3-dihydro-1H-pyrrolo[2,1-b]quinazolin-9-one		202.21	0.833	3	1	55.12	High	No
46	2,3-Dihydro-3-hydroxypyrrolo(2,1-b)quinazolin-9(1H)-one hydrochloride		238.67	1.255	3	1	55.12	High	Yes
47	Betaine		117.15	-1.557	2	0	40.13	Low	No
48	Anisotine		349.38	2.760	4	1	73.22	High	Yes
49	2',4'-Dihydroxychalcone 4'-glucoside		402.39	0.467	8	5	136.68	High	No

S.No	Compound	Structure	M. W.	Log P	HBA	HBD	TPSA	GI Abs	BBB
50	Triacontane		422.81	11.94	0	0	0	Low	No
51	Trtriacontane		464.89	13.11	0	0	0	Low	No
52	Adhatodine		335.4	3.548	3	1	53.93	High	Yes
53	Vasicine		188.23	1.296	2	1	35.83	High	No
54	alpha-Carotene		536.87	12.46	0	0	0	Low	No
55	alpha-Amyrin		426.72	8.024	1	1	20.23	Low	No

S.No	Compound	Structure	M. W.	Log P	HBA	HBD	TPSA	GI Abs	BBB
56	D-Galactose		180.16	-3.221	6	5	110.38	Low	No
57	Apigenin		270.24	3.307	5	3	90.9	High	No

MW: Molecular Weight; HBA: Hydrogen Bond Acceptor; HBD: Hydrogen Bond Donor, TPSA: Topological Surface Area; GI Abs: Gastro Intestinal Absorption; BBB: Blood Brain Barrier

**Table 3.** Toxicity was predicted for the phytochemicals of *Justicia adhatoda* using the pkCSM online web server.

S. No.	Compound	AMES toxicity	Max. tolerated dose (Log mg/kg/day)	hERG I inhibition	hERG II inhibition	Oral rat acute toxicity (mol/kg)	Oral rat chronic toxicity (Log mg/kg_bw/day)	Hepato-toxicity	Skin toxicity	CaCo <sub>2</sub> permeability (log Papp in 10 <sup>-6</sup> cm/s)
1	29-Methyl-1-triacontanol	No	-0.357	No	Yes	1.971	0.744	No	Yes	1.085
2	Flavone	Yes	0.453	No	No	1.596	0.761	No	No	1.62
3	Kaempferol	No	0.935	No	No	2.329	2.616	No	No	0.308
4	Quercetin	No	0.779	No	No	2.513	2.636	No	No	0.139
5	Luteolin	No	0.564	No	No	2.453	1.537	No	No	0.286
6	Sophoraflavonololide	No	0.478	No	Yes	2.496	4.869	No	No	-0.59
7	Daucosterol	No	-0.84	No	No	2.508	2.871	No	No	0.495
8	Octanal	No	0.614	No	No	1.655	2.084	No	Yes	1.486
9	Heptacosane	No	-0.273	No	Yes	1.764	0.967	No	Yes	1.119
10	Verbenone	No	0.526	No	No	1.861	1.873	No	Yes	1.103
11	Eicosane	No	-0.014	No	Yes	1.586	1.177	No	Yes	1.371
12	Undecanal	No	0.343	No	No	1.547	2.339	No	Yes	1.483
13	1-Tetradecanol	No	0.157	No	No	1.559	1.208	No	Yes	1.466
14	1-Octene	No	0.641	No	No	1.695	2.37	No	Yes	1.382
15	Neoandrographolide	No	-0.528	No	No	2.359	2.506	No	No	0.451
16	Quinazoline	No	0.665	No	No	2.079	2.473	No	Yes	1.838

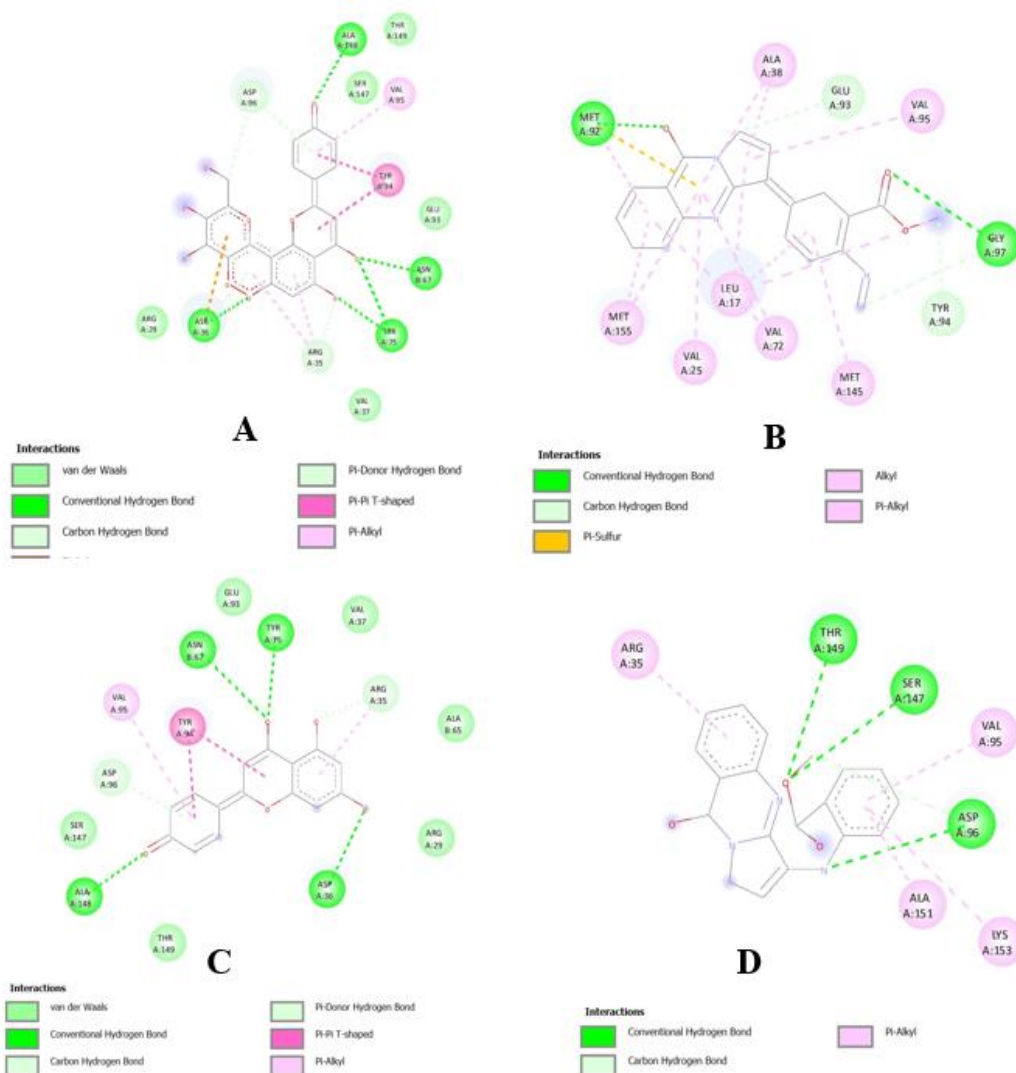
S. No.	Compound	AMES toxicity	Max. tolerated dose (Log mg/kg/day)	hERG I inhibition	hERG II inhibition	Oral rat acute toxicity (mol/kg)	Oral rat chronic toxicity (Log mg/kg_bw/day)	Hepato-toxicity	Skin toxicity	CaCo2 permeability (log Papp in 10 <sup>-6</sup> cm/s)
17	Isovitexin	No	0.745	No	Yes	3.039	3.788	No	No	0.433
18	Hentriacontane	No	-0.254	No	Yes	1.86	0.848	No	Yes	1.101
19	1-Pentadecanol	No	0.09	No	No	1.563	1.173	No	Yes	1.465
20	Pentacosane	No	-0.222	No	Yes	1.716	1.027	No	Yes	1.128
21	Heneicosane	No	-0.057	No	Yes	1.611	1.146	No	Yes	1.37
22	Nonacosane	No	-0.285	No	Yes	1.812	0.908	No	Yes	1.11
23	Tricosane	No	-0.144	No	Yes	1.663	1.087	No	Yes	1.137
24	Dodecane	No	0.324	No	No	1.566	1.45	No	Yes	1.378
25	Tetracontane	No	0.172	No	Yes	2.174	0.58	No	Yes	1.061
26	Tetradecane	No	0.221	No	No	1.527	1.377	No	Yes	1.376
27	beta-Eudesmol	No	-0.371	No	No	1.697	1.271	No	Yes	1.496
28	Ephedrine	No	0.138	No	No	2.464	1.396	Yes	Yes	1.57
29	Caryophyllene oxide	No	0.197	No	No	1.551	1.206	No	Yes	1.598
30	Phytol	No	-0.325	No	Yes	1.646	1.024	No	Yes	1.487
31	Vitexin	No	0.747	No	Yes	3.129	3.158	No	No	0.278
32	Fenretinide	No	-0.44	No	Yes	2.633	1.718	No	No	1.126
33	Desmethoxyaniflorine	No	0.09	No	Yes	2.525	1.475	Yes	No	1.264
34	3-Methyl-4-(2,6,6-trimethyl-2-cyclohexen-1-yl)-3-buten-2-one	No	0.355	No	No	1.657	1.219	No	Yes	1.515
35	Vasnetine	No	-0.376	No	Yes	2.424	1.482	Yes	No	1.222
36	7-Methoxyvasicinone	No	0.227	No	No	2.004	1.375	No	No	0.391
37	beta-Sitosterol	No	-0.555	No	Yes	2.326	0.829	No	No	1.205
38	5-Octadecenal	No	-0.074	No	Yes	1.519	1.106	No	Yes	1.483
39	Pyrrolo(2,1-b)quinazolin-9(1H)-one, 2,3-dihydro-3,7-dihydroxy-, (3S)-	No	0.246	No	No	1.813	1.331	No	No	0.661
40	Vasicinol	Yes	0.203	No	No	2.383	0.991	Yes	No	1.156
41	Deoxyvasicinone	Yes	-0.166	No	No	2.07	2.135	No	No	1.763
42	Vasicol	No	-0.14	No	No	2.41	1.209	No	No	0.403
43	Pyrrolo[2,1-b]quinazolin-9(1H)-one, 3-[2-(dimethylamino)phenyl]-2,3-dihydro-	No	-0.113	No	No	2.239	1.262	Yes	No	1.754
44	Benzenamine, N,N-dimethyl-2-(1,2,3,9-	Yes	0.127	No	Yes	2.592	0.705	Yes	No	1.654

S. No.	Compound	AMES toxicity	Max. tolerated dose (Log mg/kg/day)	hERG I inhibition	hERG II inhibition	Oral rat acute toxicity (mol/kg)	Oral rat chronic toxicity (Log mg/kg_bw/day)	Hepato-toxicity	Skin toxicity	CaCo <sub>2</sub> permeability (log Papp in 10 <sup>-6</sup> cm/s)
	tetrahydropyrrolo[2,1-b]quinazolin-3-yl)-									
45	(3S)-3-hydroxy-2,3-dihydro-1H-pyrrolo[2,1-b]quinazolin-9-one	Yes	0.037	No	No	2.101	2.368	No	No	1.227
46	2,3-Dihydro-3-hydroxypyrrolo(2,1-b)quinazolin-9(1H)-one hydrochloride	No	-0.046	No	No	2.266	1.37	No	No	1.26
47	Betaine	No	0.923	No	No	1.837	0.254	No	Yes	1.43
48	Anisotine	No	-0.356	No	Yes	2.336	1.271	Yes	No	1.219
49	2',4'-Dihydroxychalcone 4'-glucoside	No	0.128	No	No	2.282	3.245	No	No	0.244
50	Triacontane	No	-0.275	No	Yes	1.836	0.878	No	Yes	1.105
51	Tritriacontane	No	-0.185	No	Yes	1.915	0.788	No	Yes	1.092
52	Adhatodine	No	-0.499	No	Yes	2.22	0.758	Yes	No	1.317
53	Vasicine	Yes	0.18	No	No	2.671	1.243	No	No	1.611
54	alpha-Carotene	No	-0.533	No	Yes	2.201	0.6	No	No	1.24
55	alpha-Amyrin	No	-0.442	No	Yes	2.217	0.854	No	No	1.238
56	D-Galactose	No	2.071	No	No	1.018	3.32	No	No	-0.422
57	Apigenin	No	0.555	No	No	2.225	1.653	No	No	1.025

AMES toxicity: Carcinogenic (or Mutagenic) potential; hERG I & hERG II inhibition: cardio-toxicity; Oral rat chronic toxicity: log mg/kg\_bw/day; Skin toxicity: Sensitization of Skin3.2. Molecular docking

### 3.3. Screening of drug candidates for PknB.

Among the phytochemical compounds from *J. adhatoda*, the top four ligands, Vitexin, Anisotine, Apigenin, and Vasnetine, exhibited the lowest binding affinity and were considered the best. The phytoconstituents were docked in the active site of PknB and showed minimum binding energies between -10.21 kcal/mol and -8.3 kcal/mol. The 2d binding interactions of top ligands and the selected amino acids for the target protein are illustrated in Figure 1. The ligand Vitexin was found to establish five hydrogen bonds with ASP36, TYR75, ASN67, and ALA148, whereas Anisotine, the second top ligand, was found to interact with GLY97 and MET92 using two hydrogen bonds with bond distances of 2.72 and 3.05 respectively.

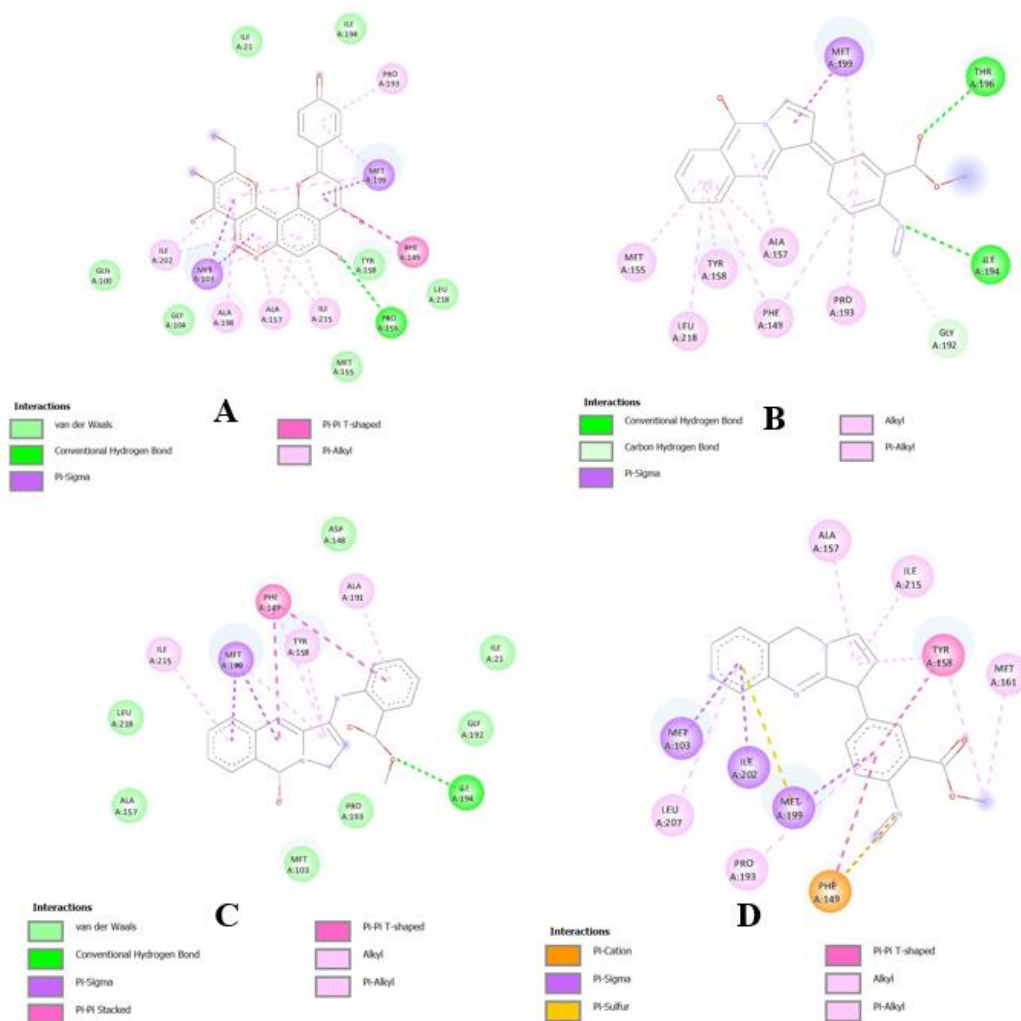


**Figure 1.** 2D interaction plot of Protein kinase B (PknB) and ligand complex visualized using Discovery Studio 2021 (A) Vitexin-PknB complex; (B) Anisotine-PknB complex; (C) Apigenin-PknB complex; (D) Vasnetine-PknB complex.

### 3.4. Screening of drug candidates for InhA.

The top four phytochemicals viz Vitexin, Anisotine, Vasnetine, and Adhatodine had the lowest binding affinity -10.23 kcal/mol, -8.99 kcal/mol, -8.97 kcal/mol, and -8.76 kcal/mol, respectively. The interactions between the top four phytochemicals and selected amino acid residues for the target protein are illustrated in Figure 2. Anisotine and Vasnetine, alkaloids from the plant *J. adhatoda*, were seen to have almost identical binding energies. Where

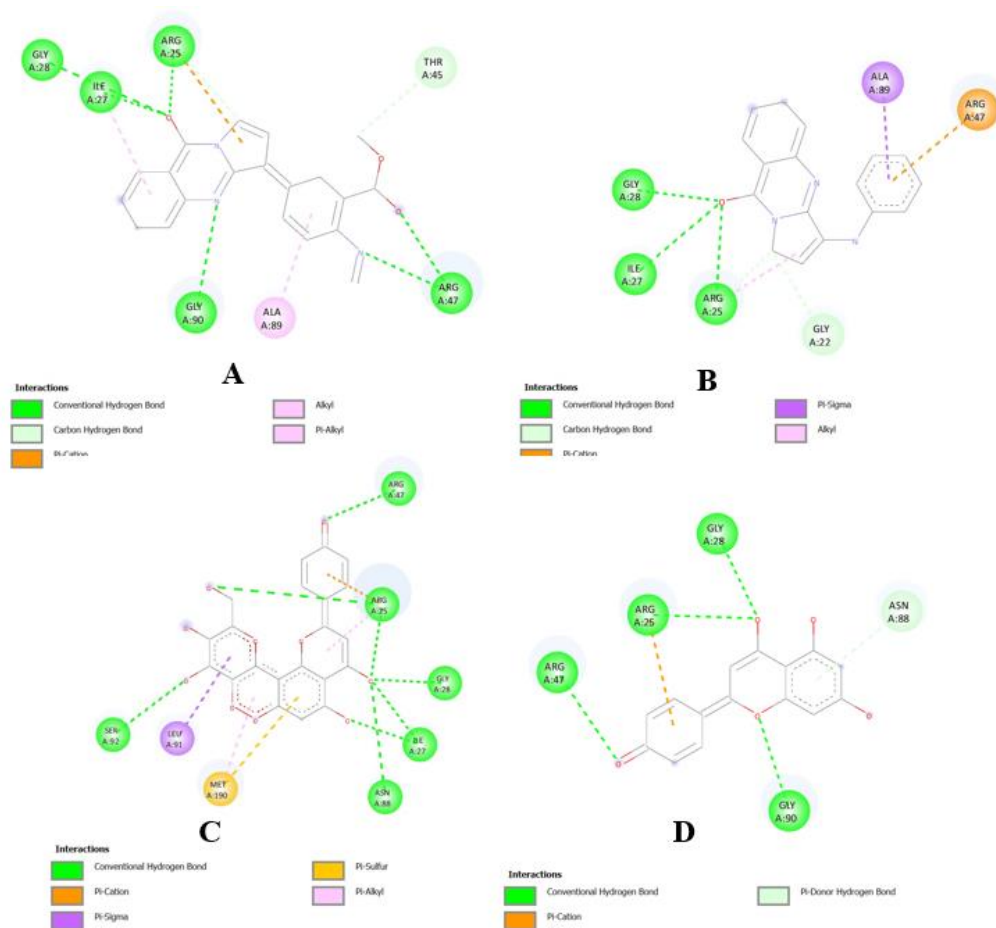
Anisotine made two hydrogen bonds with ILE194 and THR196 amino acid residues, Vasnetine was found to interact with ILE194 using a single hydrogen bond with a bond distance of 2.87.



**Figure 2.** 2D interaction plot of 2-trans-enoyl-ACP reductase (InhA) and ligand complex visualized using Discovery Studio 2021 (A) Vitexin-InhA complex; (B) Anisotine-InhA complex; (C) Vasnetine-InhA complex; (D) Adhatodine-InhA complex.

### 3.5. Screening of drug candidates for Maba.

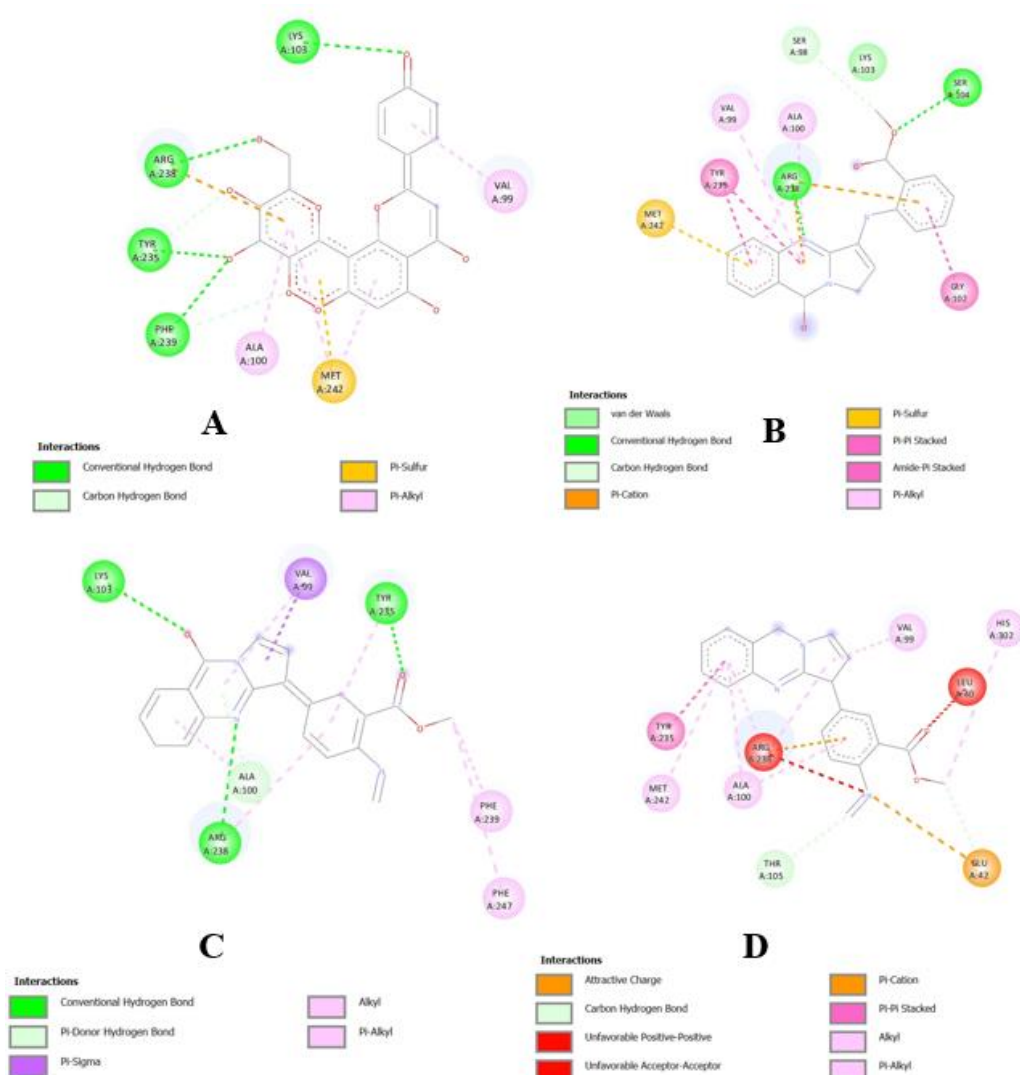
The binding affinity scores of the top four drug candidates, Anisotine, Vasnetine, Vitexin and Apigenin, were between -9.09 kcal/mol and -8.6 kcal/mol. All ligands were found to display almost similar binding scores. Anisotine with the lowest binding affinity was found to interact with GLY90, ARG47, ARG25, ILE27, and GLY28 using six hydrogen bonds, whereas Apigenin established four hydrogen bonds with GLY90, GLY28, ARG25, and ARG47 with the bond distances of 2.89, 3.02, 3.16 and 3.08 respectively. Vasnetin interacted with ARG25, ILE27, and GLY28 using three hydrogen bonds. Vasnetin protruded in the hydrophobic pocket of Maba to form strong with ALA89 and ARG47 using pi-sigma and pi-cation bonds. The interactions of ligands with the active site of Maba are shown in Figure 3.



**Figure 3.** 2D interaction plot of  $\beta$ -ketoacyl-ACP reductase (MabA) and ligand complex visualized using Discovery Studio 2021 (**A**) Anisotine-MabA complex; (**B**) Vasnetine-MabA complex; (**C**) Vitexin-MabA complex; (**D**) Apigenin-MabA complex.

### 3.6. Screening of drug candidates for PanK.

The leading four phytochemicals, namely Vitexin, Vasnetine, Anisotine, and Adhatodine, displayed a binding affinity score of -9.5 kcal/mol to -8.1 kcal/mol. Apegenin was the fifth one to show a binding affinity score of -7.54 kcal/mol. The 2D representation of all the ligands interacting in the binding pocket of PanK is shown in Figure 4. Vitexin, a flavon glucoside, and the topmost ligand, was found to interact with LYS103, ARG238, TYR235, and PHE239 using four hydrogen bonds with the bond distances of 2.76, 2.67, 3.10, and 2.44 respectively. Similarly, Vitexin and Vasnetine were found to establish four and two hydrogen bonds, respectively. Adhatodine showed no hydrogen bond interaction.

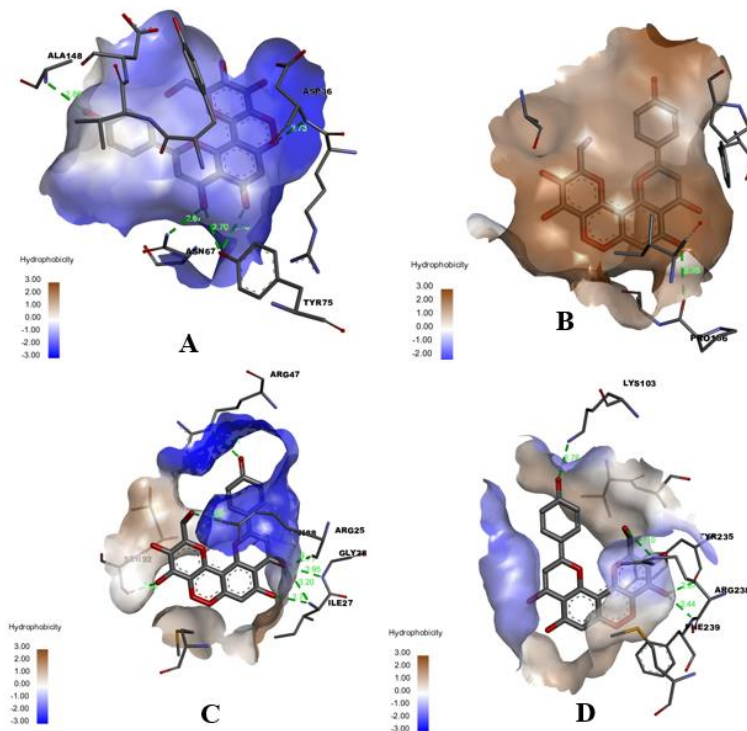


**Figure 4.** 2D interaction plot of Pantothenate kinase (PanK) and ligand complex visualized using Discovery Studio 2021 (A) Vitexin-PanK complex; (B) Vasnetine-PanK complex; (C) Anisotine-PanK complex; (D) Adhatodine-PanK complex.

### 3.7. Bioavailability radar and toxicity prediction.

Assessing bioavailability is a critical aspect of the drug development process. Low bioavailable drugs might fail to exhibit their intended therapeutic impact within the body despite having good *in vitro* properties. The SwissADME tool provides a bioavailability radar plot, which can be utilized as a means of *in silico* prediction for assessing the bioavailability of a drug [27]. Based on the binding affinity scores of the phytochemicals, the top four molecules with each receptor were chosen, resulting in the top five drug candidates. Further, these 5 drug candidates were screened based on the bioavailability and toxicity profile analysis Table 4. Vitexin, which showed the best binding affinity towards almost all of the receptors (Figure 5) and no toxicity liability, did not satisfy the bioavailability radar criteria, which has also been proved via several *in-vitro* and *in-vivo* studies [32]. To overcome the very low bioavailability of Vitexin, researchers have been working on developing nanoparticles and different analogs [33]. Vitexin has also been reported to have a range of pharmacological effects, including antioxidant, anti-inflammatory, anticancer, antinociceptive, and neuroprotective effects [34]. Anisotine is orally bioavailable as well as non-toxic and has been found to be inhibitory against SARS-CoV-2 proteins [35]. Anisotine and Vasnetine showed hepatotoxicity, whereas none of the selected compounds were found to be mutagenic (AMES toxicity). This study provides the

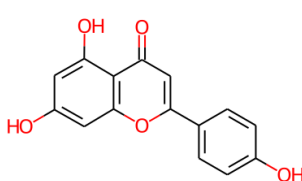
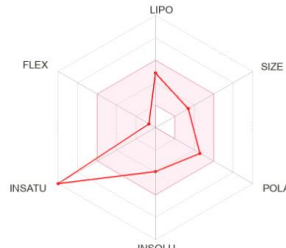
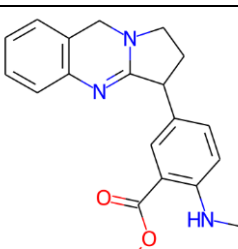
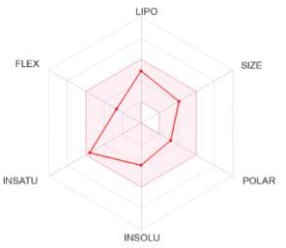
preliminary assessment of selected compounds conducted *in silico* and can complement future studies with regard to the safety and bioavailability of these compounds.



**Figure 5.** Docking pose of Vitexin within the cavity of (A) PknB; (B) InhA; (C) MabA; (D) PanK.

**Table 4.** Bioavailability radar plot along with the toxicity profile of the 5 shortlisted molecules.

Name	Structure	Bioavailability Radar	AMES Toxicity	Cardiotoxicity	Hepatotoxicity
Vitexin			Negative	Negative	Negative
Anisotine			Negative	Negative	Positive
Vasnetine			Negative	Negative	Positive

Name	Structure	Bioavailability Radar	AMES Toxicity	Cardiotoxicity	Hepatotoxicity
Apigenin			Negative	Negative	Negative
Adhatodine			Negative	Negative	Negative

#### 4. Conclusions

The global problem of the spread of MDR and XDR MTB strains leads to the exploration of novel approaches for the development of the so-called “resistance resistant” drugs. Utilizing a polypharmacology approach, phytochemicals from the plant *J. adhatoda* were screened for their antitubercular activity against PknB, InhA, MabA, and PanK, resulting in the top 5 potential molecules. These top 5 ligands, namely Vitexin, Vasnetine, Anisotine, Apigenin, and Adhatodine, displayed minimum binding energy in the range of -10.23 kcal/mol to -7.54 kcal/mol. Moreover, bioavailability and toxicity analysis of these molecules showed them to be safe and non-toxic. Hence, these compounds can be regarded as efficacious against the target proteins. The findings obtained are expected to advance therapy approaches based on traditional medicine and identify potential candidates for future lead optimization in developing anti-tubercular medications. To validate the credibility of these findings, additional steps, such as molecular dynamics simulations of the protein model and experimental studies on animal models, can be conducted. This would open up opportunities for developing highly targeted and effective therapies against MTB.

#### Funding

This research did not receive any specific grant from funding agencies.

#### Acknowledgments

The authors express their gratitude to Shaheed Rajguru College of Applied Sciences, University of Delhi, for providing the research facilities needed to conduct the study.

#### Conflicts of Interest

The authors declare that they have no conflict of interest.

#### References

1. World Health Organization. Global tuberculosis report. 27 OCTOBER 2022

- <https://www.who.int/teams/global-tuberculosis-programme/tb-reports/global-tuberculosis-report-2022>.
- Allué-Guardia, A.; García, J.I.; Torrelles, J.B. Evolution of Drug-Resistant *Mycobacterium tuberculosis* Strains and Their Adaptation to the Human Lung Environment. *Front. Microbiol.* **2021**, *12*, 612675, <https://doi.org/10.3389/fmicb.2021.612675>.
  - Tiberi, S.; Utjesanovic, N.; Galvin, J.; Centis, R.; D'Ambrosio, L.; van den Boom, M.; Zumla, A.; Migliori, G.B. Drug resistant TB – latest developments in epidemiology, diagnostics and management. *Int. J. Infect. Dis.* **2022**, *124*, S20–S25, <https://doi.org/10.1016/j.ijid.2022.03.026>.
  - Tamuhla, T.; Dave, J.A.; Raubenheimer, P.; Tiffin, N. Diabetes in a TB and HIV-endemic South African population: Analysis of a virtual cohort using routine health data. *PloS one* **2021**, *16*, e0251303, <https://doi.org/10.1371/journal.pone.0251303>.
  - Birara Aychiluhm, S.; Mohammed, E.; Altaye, H.; Urgessa, K.; Mare, K.U.; Tadesse, A.W.; Yilma, F. Tuberculosis Co-infection and Associated Factors among People Living with HIV /AIDS Who are on Antiretroviral Therapy in Pastoral Community, Northeast Ethiopia. A Bayesian Analysis Approach. *Cogent Public Health* **2022**, *9*, 2145700, <https://doi.org/10.1080/27707571.2022.2145700>.
  - Cáceres, G.; Calderon, R.; Ugarte-Gil, C. Tuberculosis and comorbidities: treatment challenges in patients with comorbid diabetes mellitus and depression. *TheR. Adv. Infect. Dis.* **2022**, *9*, 20499361221095831, <https://doi.org/10.1177/20499361221095831>.
  - Jiang, W.; Trimawartinah; Rahman, F.M.; Wibowo, A.; Sanjaya, A.; Silitonga, P.I.I.; Tang, S.; Long, Q. The co-management of tuberculosis-diabetes co-morbidities in Indonesia under the National Tuberculosis Control Program: results from a cross-sectional study from 2017 to 2019. *BMC Public Health* **2022**, *22*, 689, <https://doi.org/10.1186/s12889-022-13017-y>.
  - Alsayed, S.S.R.; Gunosewoyo, H. Tuberculosis: Pathogenesis, Current Treatment Regimens and New Drug Targets. *Int. J. Mol. Sci.* **2023**, *24*, 5202, <https://doi.org/10.3390/ijms24065202>.
  - Grüber, G. Introduction: Novel insights into TB research and drug discovery. *Prog. Biophys. Mol. Biol.* **2020**, *152*, 2-5, <https://doi.org/10.1016/j.pbiomolbio.2020.02.003>.
  - Stelitano, G.; Sammartino, J.C.; Chiarelli, L.R. Multitargeting Compounds: A Promising Strategy to Overcome Multi-Drug Resistant Tuberculosis. *Molecules* **2020**, *25*, 1239, <https://doi.org/10.3390/molecules25051239>.
  - Mishra, S.; Khatri, M.; Mehra, V. Trials and tribulations in tuberculosis research: Can plant based drug (s) be the solution. *Chem. Biol. Lett.* **2017**, *4*, 33-47.
  - Jackson, M.; McNeil, M.R.; Brennan, P.J. Progress in Targeting Cell Envelope Biogenesis in *Mycobacterium Tuberculosis*. *Future Microbiol.* **2013**, *8*, 855–875, <https://doi.org/10.2217/fmb.13.52>.
  - Antunes, S.S.; Rabelo, V.W.-H.; Romeiro, N.C. Natural products from Brazilian biodiversity identified as potential inhibitors of PknA and PknB of *M. tuberculosis* using molecular modeling tools. *Comput. Biol. Med.* **2021**, *136*, 104694, <https://doi.org/10.1016/j.combiomed.2021.104694>.
  - Sumitro, S.B. COMPUTATIONAL DOCKING STUDY OF MULTITARGET BIOACTIVE COMPOUNDS IN INDONESIA TRADITIONAL HERBAL MEDICINE FOR TUBERCULOSIS THERAPY. *Int. J. Green Pharm.* **2018**, *12*, <https://doi.org/10.22377/ijgp.v12i04.2202>.
  - Huemer, M.; Mairpady Shambat, S.; Hertegonne, S.; Bergada-Pijuan, J.; Chang, C.C.; Pereira, S.; Gómez-Mejia, A.; Van Gestel, L.; Bär, J.; Vulin, C.; Pfammatter, S.; Stinear, T.P.; Monk, I.R.; Dworkin, J.; Zinkernagel, A.S. Serine-threonine phosphoregulation by PknB and Stp contributes to quiescence and antibiotic tolerance in *Staphylococcus aureus*. *Sci. Signal.* **2023**, *16*, eabj8194, <https://doi.org/10.1126/scisignal.abj8194>.
  - Wlodarchak, N.; Feltenberger, J.B.; Ye, Z.; Beczkiewicz, J.; Procknow, R.; Yan, G.; King, T.M., Jr.; Golden, J.E.; Striker, R. Engineering Selectivity for Reduced Toxicity of Bacterial Kinase Inhibitors Using Structure-Guided Medicinal Chemistry. *ACS Med. Chem. Lett.* **2021**, *12*, 228-235, <https://doi.org/10.1021/acsmchemlett.0c00580>.
  - Mi, J.; Gong, W.; Wu, X. Advances in Key Drug Target Identification and New Drug Development for Tuberculosis. *Biomed. Res. Int.* **2022**, *2022*, 5099312, <https://doi.org/10.1155/2022/5099312>.
  - Dartois, V.A.; Rubin, E.J. Anti-tuberculosis treatment strategies and drug development: challenges and priorities. *Nat. Rev. Microbiol.* **2022**, *20*, 685–701, <https://doi.org/10.1038/s41579-022-00731-y>.
  - Björkelid, C.; Bergfors, T.; Raichurkar, A.K.V.; Mukherjee, K.; Malolanarasimhan, K.; Bandodkar, B.; Jones, T.A. Structural and Biochemical Characterization of Compounds Inhibiting *Mycobacterium tuberculosis* Pantothenate Kinase\*. *J. Biol. Chem.* **2013**, *288*, 18260–18270, <https://doi.org/10.1074/jbc.M113.476473>.

20. Arora, P. Importance of *Adhatoda Vasica* Nees In Traditional System of Medicines: A Review. *Am. J. Pharmtech. Res.* **2019**, *9*, 85-93, <https://doi.org/10.46624/ajptr.2019.v9.i2.009>.
21. Rudrapal, M.; Vallinayagam, S.; Aldosari, S.; Khan, J.; Albadrani, H.; Al-Shareeda, A.; Kamal, M. Valorization of *Adhatoda vasica* leaves: Extraction, *in vitro* analyses and *in silico* approaches. *Front. Nutr.* **2023**, *10*, 1161471, <https://doi.org/10.3389/fnut.2023.1161471>.
22. Chaudhary, N.; Mehra, V.; Mago, P.; Khatri, M. Antimycobacterial potential of Indian spices: a review. *Int. J. Pharmacognosy Phytochem. Res.* **2017**, *9*, 1127-1134, <https://doi.org/10.25258/phyto.v9i08.9620>.
23. Mishra, S.; Khatri, M.; Mehra, V. Assessing the antimycobacterial activity of the bioactive fractions of the Indian medicinal plant - *Justicia adhatoda* L. *Chem. Biol. Lett.* **2021**, *8*, 67-78.
24. Mishra, S.; Khatri, M.; Mehra, V. Inhibition of extracellular and intracellular survival of Mycobacterial strains by alkaloids extracted from *Justicia adhatoda* leaves. *Eur. J. Int. Med.* **2023**, *59*, 102241, <https://doi.org/10.1016/j.eujim.2023.102241>.
25. Gleeson, M.P.; Hersey, A.; Hannongbua, S. In-Silico ADME Models: A General Assessment of their Utility in Drug Discovery Applications. *Curr. Top. Med. Chem.* **2011**, *11*, 358-381, <https://doi.org/10.2174/156802611794480927>.
26. Daina, A.; Michielin, O.; Zoete, V. SwissADME: a free web tool to evaluate pharmacokinetics, drug-likeness and medicinal chemistry friendliness of small molecules. *Sci. Rep.* **2017**, *7*, 42717, <https://doi.org/10.1038/srep42717>.
27. Lipinski, C.A.; Lombardo, F.; Dominy, B.W.; Feeney, F.P.J. Experimental and computational approaches to estimate solubility and permeability in drug discovery and development settings. *Adv. Drug Deliv. Rev.* **1997**, *23*, 3-25, [https://doi.org/10.1016/S0169-409X\(96\)00423-1](https://doi.org/10.1016/S0169-409X(96)00423-1).
28. Morris, G.M.; Huey, R.; Lindstrom, W.; Sanner, M.F.; Belew, R.K.; Goodsell, D.S.; Olson, A.J. AutoDock4 and AutoDockTools4: Automated docking with selective receptor flexibility. *J. Comput. Chem.* **2009**, *30*, 2785-2791, <https://doi.org/10.1002/jcc.21256>.
29. Miteva, M.A.; Guyon, F.; Tuffi, P. Frog2: Efficient 3D conformation ensemble generator for small compounds. *Nucleic Acids Res.* **2010**, *38*, W622-W627, <https://doi.org/10.1093/nar/gkq325>.
30. Pires, D.E.V.; Blundell, T.L.; Ascher, D.B. pkCSM: Predicting Small-Molecule Pharmacokinetic and Toxicity Properties Using Graph-Based Signatures. *J. Med. Chem.* **2015**, *58*, 4066-4072, <https://doi.org/10.1021/acs.jmedchem.5b00104>.
31. Zhu, H.; Zhang, Y.; Li, W.; Huang, N. A Comprehensive Survey of Prospective Structure-Based Virtual Screening for Early Drug Discovery in the Past Fifteen Years. *Int. J. Mol. Sci.* **2022**, *23*, 15961, <https://doi.org/10.3390/ijms232415961>.
32. Babaei, F.; Moafizad, A.; Darvishvand, Z.; Mirzababaei, M.; Hosseinzadeh, H.; Nassiri-Asl, M. Review of the effects of vitexin in oxidative stress-related diseases. *Food Sci. Nutr.* **2020**, *8*, 2569-2580, <https://doi.org/10.1002/fsn3.1567>.
33. Li, S.; Lv, H.; Chen, Y.; Song, H.; Zhang, Y.; Wang, S.; Luo, L.; Guan, X. N-trimethyl chitosan coated targeting nanoparticles improve the oral bioavailability and antioxidant activity of vitexin. *Carbohydr. Polym.* **2022**, *286*, 119273, <https://doi.org/10.1016/j.carbpol.2022.119273>.
34. Ranjan, R.; Kishore, K.; Ranjan, R.; Sheikh, T.J.; Kumar, A.; Kumar, B.; Kumar, S.; Kumar, R. Nutraceutical potential of vitexin: a flavone glycoside. *J. Phytopharm.* **2023**, *12*, 44-50, <https://doi.org/10.31254/phyto.2023.12107>.
35. Kar, P.; Kumar, V.; Vellingiri, B.; Sen, A.; Jaishee, N.; Anandraj, A.; Malhotra, H.; Bhattacharyya, S.; Mukhopadhyay, S.; Kinoshita, M.; Govindasamy, V.; Roy, A.; Naidoo, D.; Subramaniam, M.D. Anisotine and amarogentin as promising inhibitory candidates against SARS-CoV-2 proteins: a computational investigation. *J. Biomol. Struct. Dyn.* **2022**, *40*, 4532-4542, <https://doi.org/10.1080/07391102.2020.1860133>.

**Supplementary Information****Table S1.** Minimum binding energy displayed by the top 7 phytoconstituents of *Justicia adhatoda* when docked with different protein targets (A) PknB; (B) InhA; (C) MabA; (D) PanK**(A)**

S.No.	Compound Name	Minimum Binding Energy	RUN
1	Vitexin	-10.21	6
2	Anisotine	-9.33	3
3	Apigenin	-8.34	1
4	Vasnetine	-8.3	5
5	Adhatodine	-8.16	7
6	Benzenamine, N,N-dimethyl-2-(1,2,3,9-tetrahydro pyrrolo[2,1-b]quinazolin-3-yl)-	-7.88	3
7	7-Methoxyvasicinone	-7.24	4

**(B)**

S.No.	Compound Name	Minimum Binding Energy	RUN
1	Vitexin	-10.23	5
2	Anisotine	-8.99	4
3	Vasnetine	-8.97	6
4	Adhatodine	-8.76	1
5	Benzenamine, N,N-dimethyl-2-(1,2,3,9-tetrahydropyrrolo[2,1-b]quinazolin-3-yl)-	-8.36	2
6	Apigenin	-8.36	7
7	7-Methoxyvasicinone	-6.42	7

**(C)**

S.No.	Compound Name	Minimum Binding Energy	RUN
1	Anisotine	-9.09	7
2	Vasnetine	-8.97	8
3	Vitexin	-8.75	9
4	Apigenin	-8.6	6
5	Adhatodine	-8.39	6
6	Benzenamine, N,N-dimethyl-2-(1,2,3,9-tetrahydropyrrolo[2,1-b]quinazolin-3-yl)-	-7.56	4
7	7-Methoxyvasicinone	-6.44	8

**(D)**

S.No.	Compound Name	Minimum Binding Energy	RUN
1	Vitexin	-9.5	5
2	Vasnetine	-8.99	2
3	Anisotine	-8.12	10
4	Adhatodine	-8.1	1
5	Apigenin	-7.54	8
6	Benzenamine, N,N-dimethyl-2-(1,2,3,9-tetrahydropyrrolo[2,1-b]quinazolin-3-yl)-	-7.36	2
7	7-Methoxyvasicinone	-6.51	3